PHYSICAL REVIEW B
CONDENSED MATTER

THIRD SERIES, VOLUME 28, NUMBER 11 1 DECEMBER 1983

Neutron scattering studies of the anomalous magnetic alloy $Fe_{0.7}Al_{0.3}$

K. Motoya* and S. M. Shapiro
Brookhaven National Laboratory, Upton, New York 11973

Y. Muraoka†
Department of Metal Science and Technology, Kyoto University, Kyoto 606, Japan
(Received 1 August 1983)

Small-angle total and inelastic neutron scattering measurements were performed on a single crystal of the ordered alloy $Fe_{0.7}Al_{0.3}$. The behavior of the Q dependence of the small-angle intensity can be classified into four temperature regions which correspond to the bulk behavior: (i) $T > T_c = 510$ K (paramagnetic region); the line shape is Lorentzian with $\kappa \to 0$ as $T > T_c$. (ii) 300 K $< T < T_c$ (ferromagnetic region); $I(Q) \sim Q^{-2}$ as expected from spin waves. (iii) 100 K $< T <$ 300 K (near $T_c^{\rm inv}$); $I(Q) \sim Q^{-\alpha}$, with α being T dependent and reaching a maximum value $\alpha = 2.6$. In this region the T dependence of the intensity exhibits a peak which is Q dependent. Near $T_c^{\rm inv} \approx 160$ K, a thermal hysteresis and novel time dependence of the scattering is observed. (iv) $T < 100$ K (spin-glass regime); the line shape is again Lorentzian with κ increasing with decreasing T. No anomaly is observed at $T_f \approx 90$ K. The inelastic measurements reveal that spin waves exist in the ferromagnetic regime but disappear as the temperature is lowered. For temperatures less than $T_c^{\rm inv}$, an elastic central peak appears which increases as T is decreased. The results are interpreted in terms of random-field effects.

I. INTRODUCTION

Some concentrated magnetic alloys exhibit a peculiar sequence of phase transitions. Based upon calculations for an Ising system with infinite-range random interaction the theory predicted a transition from a paramagnetic (PM) state to a ferromagnetic (FM) state at $T = T_c$. At a lower temperature, $T = T_f$, the ferromagnetism disappears and a spin-glass (SG) state is present.[1] In actual magnetic systems, however, the nature of low-temperature "spin-glass-like" phase, and even the FM state, have not been fully clarified. These so-called reentrant spin-glasses (RSG's) encompass a wide variety of materials including crystalline alloys $(PdFe)_{1-x}Mn_x$,[2] $Fe_{1-x}Cr_x$,[3] amorphous alloys $(Fe_{1-x}Mn_x)_{75}P_{16}B_6Al$,[4] $(Fe_{1-x}Ni_x)_{75}P_{16}B_6Al_3$,[5] and the ionic crystal $Eu_{1-x}Sr_xS$.[6]

The Fe-Al alloy is also a member of this group of materials but susceptibility and magnetization measurements demonstrate a more complicated behavior in the concentration range near $Fe_{0.7}Al_{0.3}$. The disappearance of ferromagnetism in the Fe-Al alloy upon decreasing temperature was observed by Arrott and Sato[7,8] in 1959, long before the discovery of SG's. They observed that the spontaneous magnetization in a $Fe_{0.696}Al_{0.304}$ alloy continuously decreased as the temperature was lowered below room temperature and finally disappeared below 180 K. They suggested the occurrence of a phase transition from a FM phase at high temperature to an antiferromagnetic phase at lower temperature.

Kouvel[9] observed a displaced hysteresis loop and a large $\sin\psi$ variation of a torque curve measured on a field-cooled $Fe_{0.7}Al_{0.3}$ sample. He suggested that a magnetic field alters the magnetic order of the coexisting ferromagnetic and antiferromagnetic spin alignment. However, an early neutron-diffraction measurement[10] found no evidence for an antiferromagnetic order above 4.2 K for alloys in the concentration range 33—50 at.% Al. Shull *et al.*,[11] through their extensive alternating low-field susceptibility and steady-field magnetization measurements, characterized a relation between phase transitions and composition as well as atomic ordering in an Fe-Al alloy system.

The Fe-Al alloy with the composition near $Fe_{0.7}Al_{0.3}$ exhibits two kinds of atomic order.[12–14] In a FeAl-type—order alloy, all corner sites are occupied by iron atoms (β sites) and body-centered sites are occupied randomly by iron or aluminum atoms. In the Fe_3Al-type order a unit cell includes eight body-centered cubic subcells,

with all corner sites of subcells occupied by iron atoms and each body-centered site is alternately occupied by an aluminum atom or an Fe atom (α sites). For the Al-rich alloy, the iron body-centered site contains a distribution of Fe and Al occupancies.

In Fig. 1(b), the phase diagram for Fe_3Al-type—order alloy is schematically illustrated. The most remarkable result is the complicated characteristic of the alloy near $Fe_{0.7}Al_{0.3}$ composition, which is the subject of the investigation reported in the present paper. As seen in the magnetization measurements in Fig. 1(a), a $Fe_{0.7}Al_{0.3}$ alloy with Fe_3Al-type order transforms from a paramagnetic to a FM phase near $T_c \approx 400$ K and then from the FM state back to a PM phase at $T_c^{inv} \approx 170$ K. Finally, at $T_f = 92$ K it transforms into a SG-like state. There are some observations which suggest that the FM phase is somewhat marginal in zero external field. For example, the low alternating field susceptibility is not as high as the value for the Fe-rich ferromagnetic alloy.[11] The Mössbauer spectrum[15] of $Fe_{0.702}Al_{0.298}$ at 295 K is also different from that of a normal ferromagnet.

Diffuse neutron scattering and polarized neutron-diffraction measurements on the $Fe_{0.7}Al_{0.3}$ alloy (Fe_3Al-type order) have been performed by Cable *et al.*[16] The diffuse scattering intensity measured at $Q = 0.148$ Å^{-1} varies strongly with temperature but it shows no anomaly either at T_c^{inv} or at T_f. This suggested that FM clusters exist throughout all of the temperature region (10—500 K) and that the magnetic transitions result from the manner of the coupling of clusters. The decrease in small-Q cross section by applying magnetic field was interpreted as due to the alignment of clusters. From the flipping-ratio measurement Cable *et al.*[16] determined the field and temperature dependence of magnetic moment values for two kinds of Fe atomic positions. They proposed a model describing the relation between the moment value and the local atomic environment. They further argued that the alloy tends to cluster into two kinds of regions whose diameters are approximately 25 Å and that the antiferromagnetic interaction across the cluster boundary might cause the magnetic transitions.

The temperature dependence of small-angle neutron scattering on the same alloy has been studied by Child.[17] The Q regime probed was much smaller than that of Cable *et al.*[16] He observed a peak in the critical scattering around $T_c \approx 490$ K, in addition to another peak near T_c^{inv}, whose position shifts with Q from 200 K for $Q = 6.7 \times 10^{-3}$ Å^{-1} to 184 K for $Q = 20.1 \times 10^{-3}$ Å^{-1}, but there was no change in the intensity at T_f. The Q dependence of the scattered intensity could be described by the square of a Lorentzian. The correlation range of the clusters exhibited a minimum of 60 Å at 160 K and reached values of 150 Å at 9 and 300 K. The external field dependence of scattered intensity suggests that the magnetic scattering is very sensitive to the field even in the FM phase.

We report on a small-angle neutron scattering (SANS) study on our single crystal of $Fe_{0.7}Al_{0.3}$ in order to examine in more detail the temperature and spatial dependence of the spin correlations. Inelastic scattering measurements are also reported in order to probe the spin dynamics of this material. A preliminary result of the present work has already been reported.[18]

In this paper, sample characteristics and experimental detail are described in Sec. II. Results and analysis are presented in Sec. III. In Sec. IV a discussion of the results is presented.

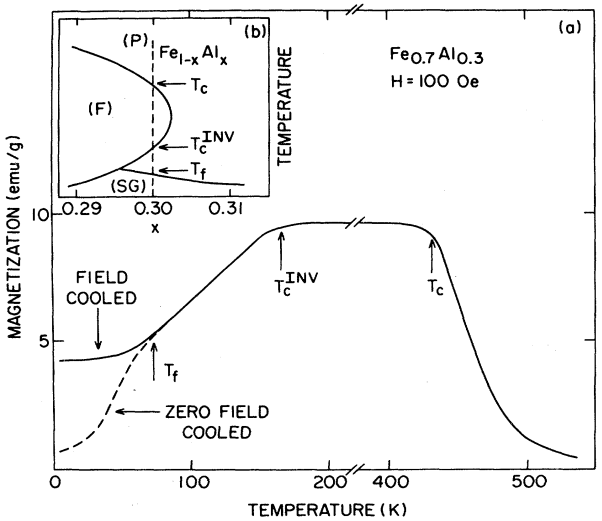

FIG. 1. (a) Temperature dependence of magnetization of $Fe_{0.7}Al_{0.3}$ measured in the field of 100 Oe. (b) Schematic magnetic phase diagram of $Fe_{1-x}Al_x$ alloy near $x = 0.3$.

II. EXPERIMENTAL DETAILS

A. Sample

A single crystal of nominal composition of $Fe_{0.7}Al_{0.3}$ was grown by the Bridgman technique, homogenized at 1100 °C for 3 d, then annealed at 700 °C for a day in order to achieve FeAl-type atomic order. The FeAl-type order was chosen after the suggestion by Shull *et al.*[11] that it is possible to have both wider composition and temperature range for the intermediate paramagnetic phase than the alloy of Fe_3Al-type order.

The composition was determined from the saturation magnetization value at room temperature for two small tips cut from upper and lower sides of the grown crystal. The magnetization was compared to that measured by Shull *et al.*[11] Values of 30.2 and 30.0 at. % Al were obtained, which assure us that the composition distribution in the sample during crystal growth, is less than 0.2% and that the average composition is very close to the nominal value. The crystal, mounted with a [110]-direction vertical, had a mosaic of $\sim 1°$ in the horizontal plane, but a much larger value perpendicular to the scattering plane. This made it difficult to perform measurements near a Bragg peak. The sample size was $\sim 5 \times 10 \times 15$ mm^3, and the lattice parameter for our sample was $a = 5.7912$ Å at room temperature. The temperature variation of the magnetization was measured under the steady field of 100 Oe.

The behavior shown in Fig. 1(a) is essentially the same as the previously reported result.[11]

From this measurement, the three transition temperatures present in our sample were determined to be $T_c \approx 430$ K, $T_c^{\text{inv}} \approx 160$ K, and $T_f \approx 70$ K. A shift of T_c to higher temperature was experienced during the prolonged neutron scattering measurements above 600 K. This suggests that the atomic order changed to somewhere between FeAl- and Fe_3Al-type order. The T_c finally determined from neutron scattering data is 510 K.

B. Neutron scattering

Neutron scattering measurements were performed using two kinds of spectrometers both installed at the cold neutron facility of the Brookhaven High Flux Beam Reactor. Small-angle total (energy-integrated) scattering intensity was measured using the SANS facility of the Brookhaven Biology Department. An incident-neutron energy of 3.33 meV ($\lambda = 5$ Å) was selected by an Fe-Mn multilayer and beam collimation before the sample was determined by two 4-mm-diam apertures separated by 1.5 m. The scattered neutrons were detected by an 18×18 cm^2 area detector placed about 2 m behind the sample. The momentum transfer range of $0.008 \lesssim Q \lesssim 0.065$ Å^{-1} was covered.

The inelastic scattering measurements were performed on a high-resolution triple-axis (double-crystal monochromator) spectrometer. Pyrolytic grapite was used both for monochromators and analyzer. A cooled beryllium filter was placed before the monochromators to eliminate the higher-energy neutrons. Most of the measurements were made in constant-Q scan mode with a fixed final neutron energy of 2.5 meV, which gives an energy resolution of ~ 30 μeV [full width at half maximum (FWHM)]. Because of the high resolution required and the poor mosaic, it was not possible to measure about a Bragg peak, so measurements were performed near the forward direction. This was also advantageous since it avoided the intense phonon scattering contributions present near Bragg peaks. The sample was mounted either in a closed-cycle refrigerator or in a conventional air-cooled furnace.

III. RESULTS AND ANALYSIS

A. Small-angle scattering

The small-angle scattering pattern taken with the incident-beam direction being nearly parallel to the [100] and with [110] vertical was isotopic. Therefore the intensity was summed over a series of rings and normalized by the area of an individual ring. The temperature variation of the scattered intensity at several Q values is shown in Figs. 2(a) and 2(b). Two sets of measurements were performed in the Displex refrigerator and the furnace and the results were normalized at $T = 300$ K. The general behavior of the intensity is similar to that previously reported by Child.[17] The intensity drops rapidly above T_c and a peak appears at lower temperatures, whose position at the smallest Q curve nearly corresponds to T_c^{inv}, as determined by bulk measurements, but it shifts to lower

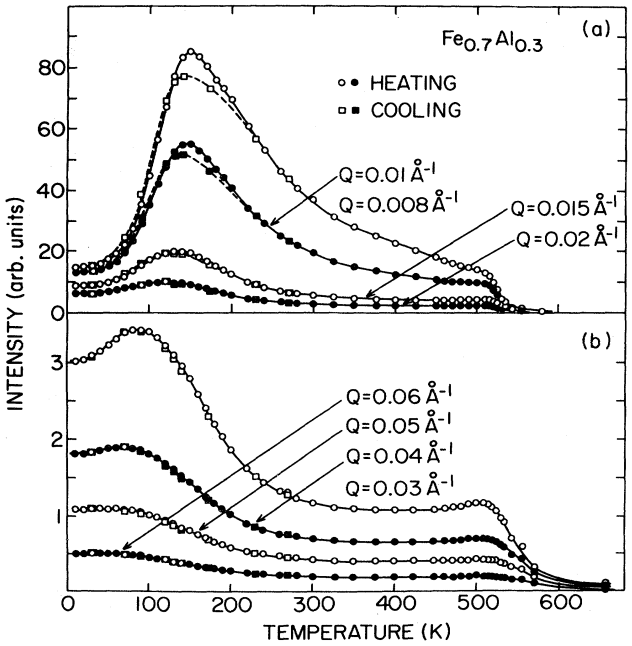

FIG. 2. Temperature dependence of small-angle total neutron scattering intensity from $Fe_{0.7}Al_{0.3}$. Circles and squares correspond to the points taken on heating and cooling processes, respectively. Statistical error is smaller than the size of marks.

temperature as Q increases. The differences of T_c and T_c^{inv} between the present result and Child's are probably due to slight differences of composition and atomic order. No anomaly is observed in the scattered intensity near T_f within the Q range covered in the present experiment. In the present measurement, however, a pronounced thermal hysteresis effect was observed below room temperature. This will be described in detail in the final part of this section.

In Fig. 3 the Q dependence of the scattered intensity is shown for several temperatures by plotting the inverse of the intensity as a function of Q^2. In this plot the intensity at the higher temperature (655 K) has been subtracted from the individual data. This implies that the scattering at this temperature is all nonmagnetic, arising from nuclear incoherent scattering from the sample and the walls of the furnance.

The temperature dependence of the intensity can be classified into four regions as shown in Figs. 2 and 3.

(i) $T > T_c = 510$ K, the scattered intensity follows the Ornstein-Zernike form

$$I(Q) = A/(\kappa^2 + Q^2), \quad T > 510 \text{ K} \tag{1}$$

for $Q \lesssim 0.045$ Å^{-1}, where B and κ are the scattering amplitude and the inverse correlation length $\kappa = \xi^{-1}$, respectively.

(ii) In the high-temperature part of FM phase 300 K $< T < T_c$ the κ is essentially zero and the intensity follows the relation

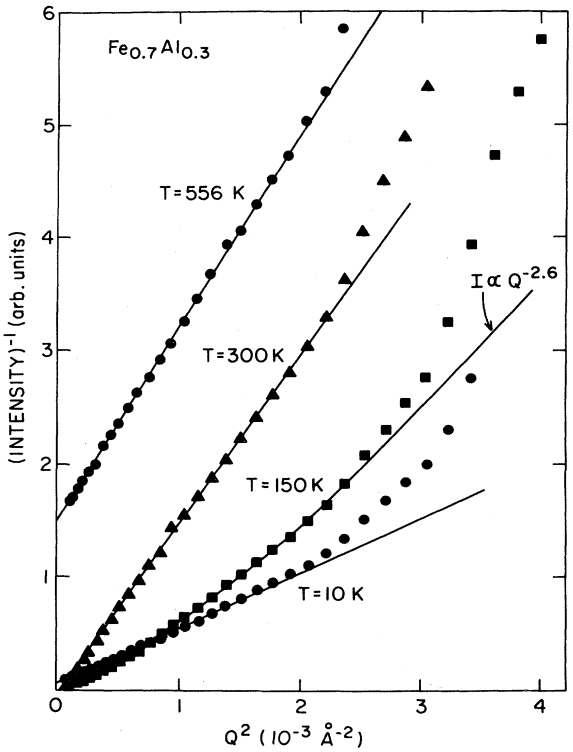

FIG. 3. Inverse intensity vs square of momentum transfer at various temperature for $Fe_{0.7}Al_{0.3}$. Scattering intensity at 655 K is subtracted from the data as a background.

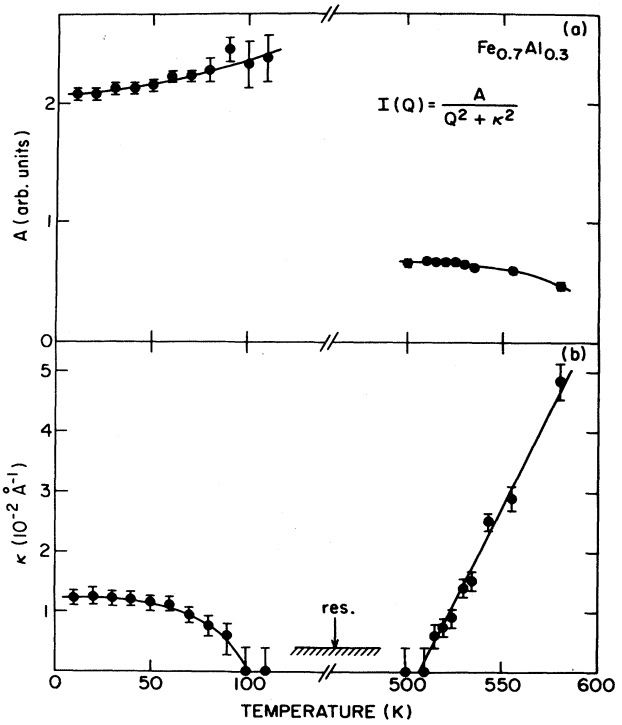

FIG. 4. Temperature dependence of (a) amplitude of scattering intensity and (b) inverse correlation length for $Fe_{0.7}Al_{0.3}$.

$$I(Q)=B/Q^2\,,\quad 300<T<510\ \text{K} \tag{2}$$

for $Q\lesssim 0.045$ Å^{-1}.

(iii) $\widetilde{100}<T<300$ K. As the temperature is lowered toward T_c^{inv}, the deviation from Eq. (2) appears and the Q dependence is approximately represented by a power law,

$$I(Q)=B/Q^{-\alpha}\,,\quad 100<T<300\ \text{K} \tag{3}$$

with a temperature-dependent exponent α.

(iv) For $T<T_f$ the behavior of the intensity again follows the Lorentzian form of Eq. (1) with a finite κ. At any temperature the deviation from theoretical forms was observed for $Q\gtrsim 0.045$ Å^{-1}. This is probably due to the inadequate subtraction of background.

In Fig. 4 the temperature variations of scattering amplitude A and inverse correlation length κ are shown in temperature regions (i) and (iv) where a Lorentzian describes the data. Figure 5 shows the temperature variations of parameters α and B in Eq. (3) for regions (ii) and (iii) where $\kappa=0$. The results were obtained from the best fit within $0.01\leq Q\leq 0.046$ Å^{-1}. The temperature range is extended beyond the regions described above in order to show the gradual entry into this region. In the region above $T_c=510$ K, the inverse correlation length approaches 0 as $T\to T_c$. This demonstrates that the material behaves as a normal ferromagnet above T_c although the behavior in the immediate vicinity of T_c has not been studied in detail in the present experiment. Also in the FM phase, the scattering follows the form as is expected from a spin-wave contribution in normal ferromagnets except for the temperature region close to T_c^{inv}. In region (ii) we can set a lower limit of 250 Å to the size of the correlation length. The deviation from the relation of Eq. (2) expected for spin waves has also been observed in other RSG materials,[3,19,20] although they transform directly to an SG phase without the intermediate PM phase. This

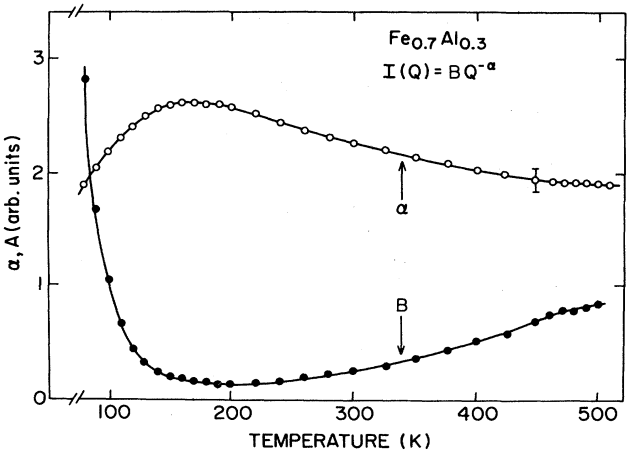

FIG. 5. Temperature dependence of exponent α and amplitude A in power-law scattering form for $Fe_{0.7}Al_{0.3}$.

behavior has been interpreted[20] as the result of increasing contribution of a Lorentzian-squared form of the "order-parameter" scattering originating from the break up of the large FM clusters due to random-field effects.[21–25] The superposition of spin-wave scattering with the form of Eq. (2) and the

$$I(Q)=C\kappa/(\kappa^2+Q^2)^2 \tag{4}$$

form with small κ value is well approximated by Eq. (3), and the relative weight of each contribution determines the parameter α. The temperature variation of α shows that the contribution from the order-parameter term reaches its maximum around $T_c^{\rm inv}$.

The appearance of a finite inverse correlation length below $T_c^{\rm inv}$ followed by its gradual increase as the temperature decreases suggests a freezing of correlated spins into finite-size clusters. This behavior has also been observed in other SG systems.[3,20,26]

We will now describe the time-dependent scattering behavior and the thermal hysteresis effect observed near $T_c^{\rm inv}$. The small-angle scattering measurements of Fig. 2 were normally performed by counting for 1 h and then changing the temperature by about 10 K to the new point. 15 min were allowed for the sample to come to equilibrium and the count was started. The hysteresis observed in Fig. 2 was measured by this method. It was noted that if we stayed at 150 K and counted repeatedly the intensity gradually decreased and approached the cooling curve. In order to explore this more quantitatively we quickly heated the sample from 10 to 150 K (within about 15 min) and the scattered intensity was repeatedly counted in 26-min intervals. The surprising result is that the time dependence is Q dependent as shown in Fig. 6. We took the intensity level after 400 min as the equilibrium baseline in order to plot the curve in Fig. 6. The intensity change ΔI follows an exponential form

$$\Delta I \sim \exp(-t/t^*)\ , \tag{5}$$

where the characteristic time t^* is a function of Q (and probably also of temperature). The solid line in Fig. 6 is the result of a fit of Eq. (5) with t^* being the adjustable parameter. A semilog plot of t^* vs Q^2 is shown in Fig. 7. This behavior of t^* with Q is consistent with our data, but does not rule out another form of the Q dependence. In the discussion below we will justify the chosen Q dependence of t^*.

B. Inelastic scattering

Inelastic neutron scattering measurements were performed around the (0,0,0) reciprocal-lattice point, i.e., the forward direction, and the direction of momentum transfer was nearly parallel to the [110] direction. Data were taken at momentum transfer of $0.05 \le Q \le 0.10$ Å^{-1}. Scattering spectra for $Q=0.06$ Å^{-1} at some representative temperatures are shown in Fig. 8. At 295 K, well-defined spin-wave peaks are present in addition to a quasielastic central component. As the temperature is decreased to 250 K, spin-wave peaks become less pronounced due to a decrease in energy and a broadening, and

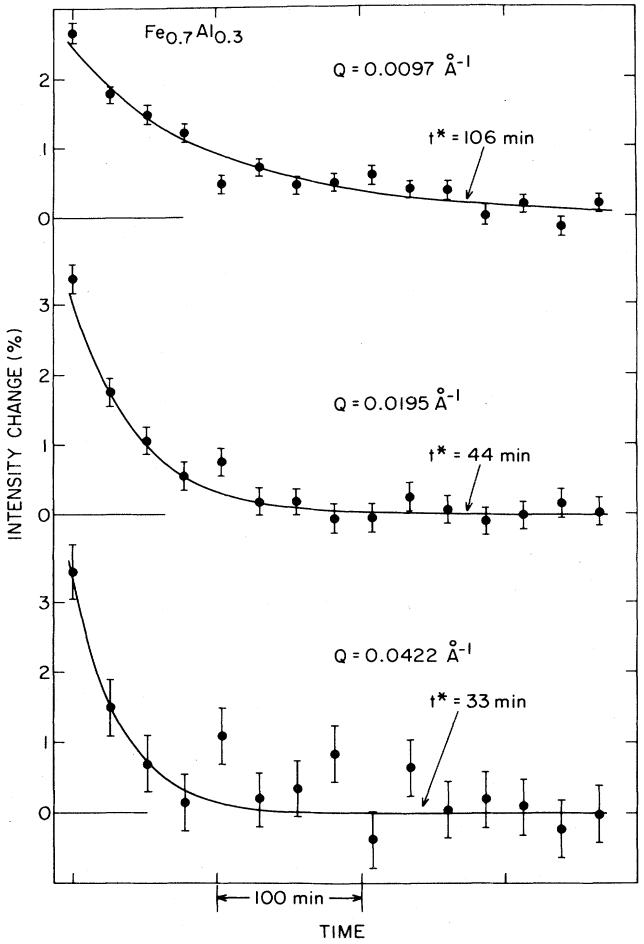

FIG. 6. Time evolution of scattering intensity at 150 K after being quickly heated from 10 K for $Fe_{0.7}Al_{0.3}$. Curves represent an exponential decay form with characteristic t^*.

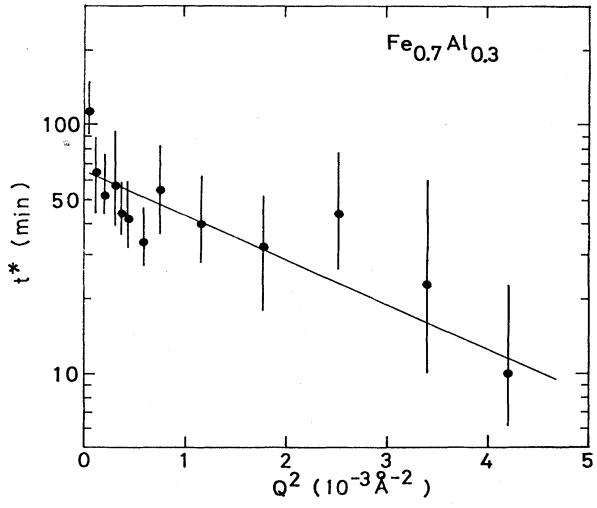

FIG. 7. Semilog plot of characteristic time t^* vs Q^2 for intensity evolution at 150 K after being quickly heated from 10 K.

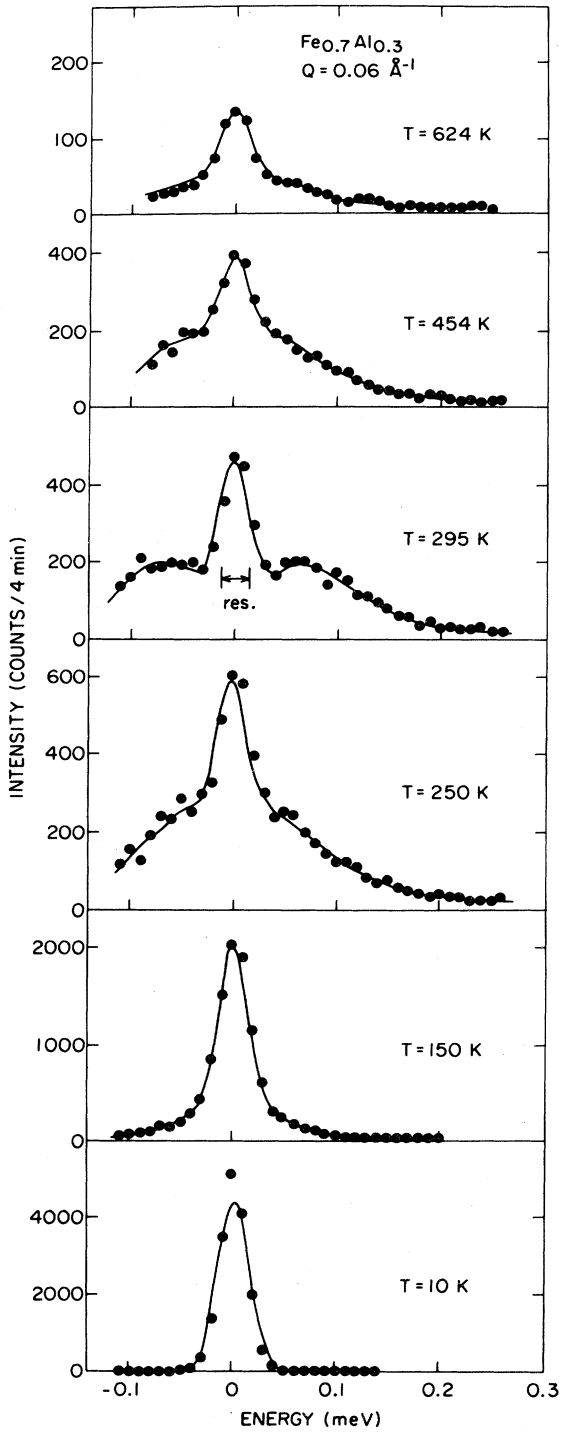

FIG. 8. Neutron scattering spectra for $Fe_{0.7}Al_{0.3}$ at several temperatures measured at $Q=0.06$ Å^{-1}. Curves are fits to the data as described in the text.

finally fade into the tails of the quasielastic component as seen in the spectrum at 150 K. Below $T\approx T_c^{\rm inv}$, the scattering spectrum is composed by a resolution-limited sharp component and a broad quasielastic part both centered at $E=0$. Intensity of the former component increases while that of the later component decreases as temperature is decreased and finally the spectrum at 10 K consists of only the resolution-limited quasielastic peak.

In order to analyze these results we follow the procedure used in previous studies of similar systems.[27,28] The scattering cross section from a ferromagnet can be written as

$$\frac{d^2\sigma}{d\Omega\, d\omega}=A\frac{k_f}{k_i}\frac{\hbar\omega/kT}{1-\exp(-\hbar\omega/kT)}\times\chi_0^{-1}[\tfrac{2}{3}\chi_Q^t F^t(Q,\omega)+\tfrac{1}{3}\chi_Q F^l(Q,\omega)]\,. \quad (6)$$

The coefficient contains some trivial constants including the magnetic form factor $f(Q)$ which is near unity at these small momentum transfers. k_f and k_i are the final and initial wave vector of the neutron and χ_0 is the susceptibility of an isolated ion which varies as $\chi_0\sim T^{-1}$. The superscripts t and l refer to the transverse and longitudinal parts of the susceptibility. Since we are dealing with mainly spin waves below T_c, we concern ourselves only with χ_Q^t which behaves as $\chi_Q^t\sim Q^{-2}$ for small Q. The cross section for spin waves in a ferromagnet becomes

$$\frac{d^2\sigma}{d\Omega\, d\omega}=A_S\frac{k_f}{k_i}\frac{\hbar\omega/kT}{1-\exp(-\hbar\omega/kT)}\frac{F_S(Q,\omega)}{Q^2}\,, \quad (7)$$

with $A_S\sim T$.

$F(Q,\omega)$ is the spectral-weight function and we assume that the observed spectrum due to spin waves can be characterized by a double Lorentzian centered at $E=\pm\hbar\omega_Q$,

$$F_s(Q,\omega)=\frac{1}{2}\left[\frac{\Gamma_Q}{(\omega-\omega_Q)^2+\Gamma_Q^2}+\frac{\Gamma_Q}{(\omega+\omega_Q)^2+\Gamma_Q^2}\right], \quad (8)$$

where Γ_Q is the halfwidth at half maximum (HWHM) of the spin-wave excitation. In order to take into account of the existence of a central peak we add to Eq. (7) a δ function centered at $E=0$. The final form of the cross section is

$$\frac{d^2\omega}{d\Omega\, d\omega}=A_S\frac{k_f}{k_i}\frac{\hbar\omega/kT}{1-\exp(-\hbar\omega/kT)}\frac{F_S(Q,\omega)}{Q^2}+\frac{A_G}{Q^2}\delta(\omega)\,, \quad (9)$$

where A_G and A_S are the integrated intensities of the spin-wave part and the elastic part, respectively. The cross section of Eq. (9) is convoluted with instrumental resolution function and the parameters A_S, A_G, ω_Q, and Γ_Q in Eqs. (7)–(9) are determined by the least-squares-fitting procedure to the observed spectra. Curves in Fig. 8 represent fits to the data using the above procedure and, as can be seen, the fits are reasonable. Figures 9(a) and 9(b) show the Q dependence of linewidth and spin-wave energy at two temperatures. Spin-wave energy follows a relation

$$\hbar\omega_Q=\Delta+DQ^2\,, \quad (10)$$

where D is the spin-wave stiffness constant and Δ is the

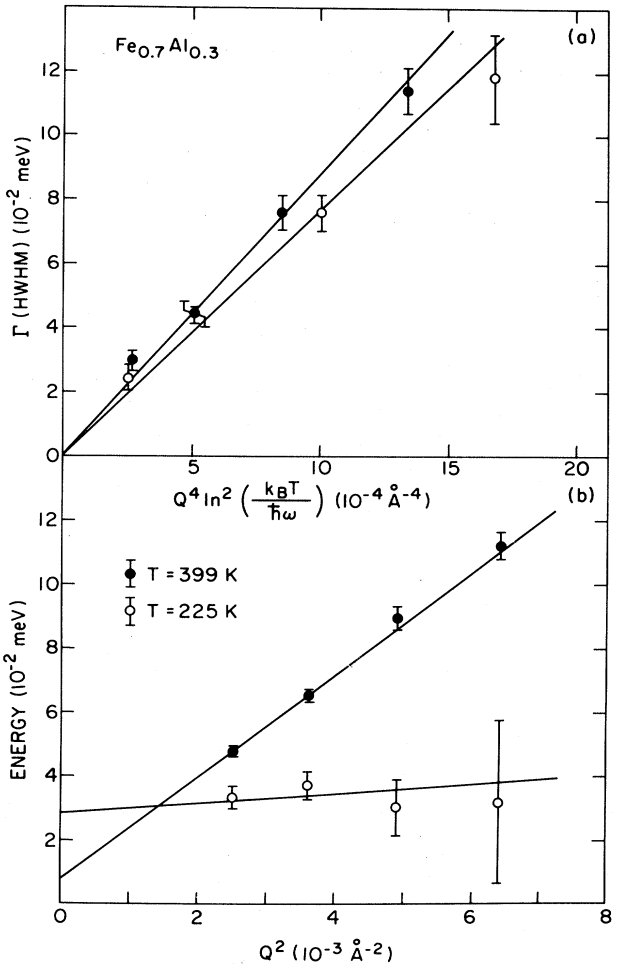

FIG. 9. (a) Spin-wave linewidth Γ as a function of $Q_4 \ln^2 (k_B T/\hbar\omega)$. (b) Spin-wave energy for $Fe_{0.7}Al_{0.3}$ as a function of Q^2 at 225 and 399 K.

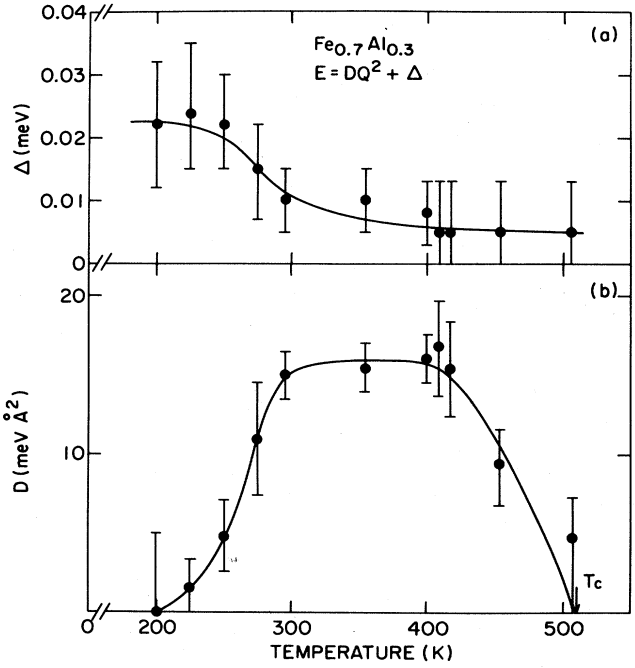

FIG. 10. Temperature dependence of (a) spin-wave gap and (b) spin-wave stiffness for $Fe_{0.7}Al_{0.3}$.

spin-wave gap due to anisotropy. The linewidth Γ follows the prediction of spin-wave theory,[29]

$$\Gamma(Q) \sim T^2 Q^4 \ln^2 \left[\frac{kT}{\hbar\omega_Q} \right] . \tag{11}$$

In Fig. 10 the temperature variation of spin-wave stiffness D and spin-wave gap Δ are shown. The stiffness increases below T_c, as expected in a ferromagnet, and reaches a maximum of 16 meV $Å^{-2}$ below 400 K and then decreases again below 300 K. No propagating features are discernible below 200 K. This feature has already been observed in several RSG's.[19,28,30] It also appears that the spin-wave gap energy Δ increases. This would be interesting since recent arguments report a need for anisotropy in order to have a SG phase.[31] However, the spin waves in this regime are very broad and parameters in the fit become correlated. The temperature-dependent behavior of Δ should therefore be treated with caution and deserves further investigation. Below $\sim$150 K the width of Lorentzian centered at $E=0$ continues to increase as the temperature decreases down to 10 K. The width of the Gaussian quasielastic central component is resolution limited over the entire temperature region.

Figure 11 shows the temperature variation of integrated intensity for the spin-wave part A_S and the resolution-limited quasielastic part A_G for $Q=0.06$ $Å^{-1}$. The dashed curve shows the observed total scattering measured in the SANS experiment in Fig. 2. It is seen that the sum A_S+A_G is essentially the same as that observed in the

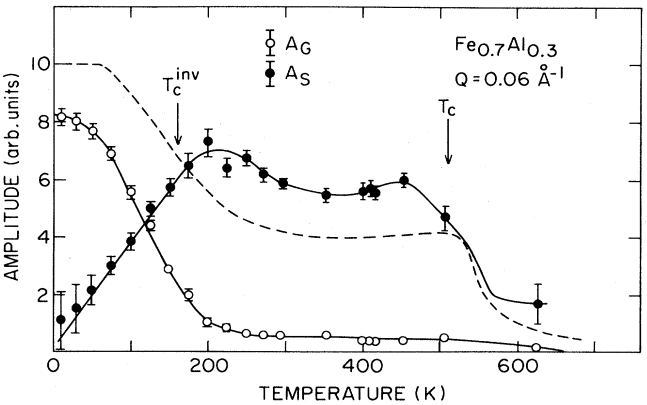

FIG. 11. Temperature dependence of relative amplitude of quasielastic scattering A_G and spin-wave scattering A_S in $Fe_{0.7}Al_{0.3}$ as determined for Eq. (10). Dashed curve shows the observed total scattering intensity measured in the SANS experiment Fig. 2. Solid curves are drawn to guide the eye.

SANS experiments. Figure 11 shows that above $T=200$ K spin-wave scattering is the dominant contribution, whereas below 200 K the central peak increases and becomes the dominant contribution to the total intensity as the temperature is further decreased.

IV. DISCUSSIONS

The present neutron scattering experiment provides us with information about the spatial and temporal properties of $Fe_{0.7}Al_{0.3}$ which, taken with other measurements, begins to describe the anomalous temperature-dependent behavior occurring in this alloy. The bulk measurements[11] have shown that the magnetization disappears as the temperature is lowered below 200 K. The decrease in the magnetic stiffness below 300 K and its disappearance as T approaches 200 K also suggests that the magnetization is dissolving as T decreases. This is an unusual phenomenon, but is now documented to occur in many alloys where competing interactions and frustration play an important role.[2–4,6,20,27] The driving mechanism proposed to cause this breakup of magnetic order is the internally generated random fields.[20,26] These have been described as a random molecular field due to the freezing of spins which do not participate in the ferromagnetism at the intermediate temperatures. The spins belong to isolated clusters which have never actually been observed, but it is highly probable that they are present. In the Fe-Al alloy studied here, their presence is on firmer ground. This was pointed out by Cable *et al.*[16] who demonstrated that the local environment has a strong effect on the magnetic moment of the iron atom. The α-site Fe atom with more than four iron near neighbors n has a relatively large $[(1.4–2.2)\mu_B]$ local moment whereas if there are less than four Fe near neighbors, the moment is greatly reduced. It was shown that $Fe_{0.7}Al_{0.3}$ alloy divides itself into regions which have $n>4$ that can support ferromagnetism and regions of $n<4$ which are paramagneticlike. These latter clusters are the origin of the random fields that destroy the ferromagnetism.

Accepting the existence of random fields we now describe the temperature-dependent behavior of $Fe_{0.7}Al_{0.3}$. The ideas are essentially the same as applied to the amorphous system $(Fe_{1-x}Mn_x)_{75}P_{16}B_6Al_3$ which exhibits behavior similar to that observed here.[20,28] $Fe_{0.7}Al_{0.3}$ alloys consist of regions which by themselves would order ferromagnetically at T_c^0 determined by the local environment and other regions which are paramagnetic at high temperatures but would order into a SG phase at T_f^0 due to competing exchange interactions possibly from a Ruderman-Kittel-Kasuya-Yosida (RKKY) form of the exchange. In the high-temperature FM phase, the fluctuations of the spins in the PM clusters are so rapid that the FM network is less influenced by them and their effect is only to reduce the net FM moment. The long-wavelength spin waves are hardly affected. This occurs in region (ii) between T_c and 300 K where the spin waves exhibit more or less normal FM behavior (see Fig. 10). The Q dependence of the scattering follows $I(Q)\sim Q^{-2}$ (Figs. 3 and 4) as is expected from spin waves. Also, from an energy analysis of the scattering, most of the intensity is due to spin waves and the central peak intensity is independent of temperature and due to the nonmagnetic background (Fig. 11).

On decreasing the temperature toward $T_c^{\rm inv}$ [region (iii)], the thermal fluctuations of the spins in the paramagnetic clusters become slower. Now the coupling between these spins and the FM network becomes important and the molecular field from the slow PM spins acts as a random magnetic field. This causes a breakup of the FM network into finite-sized clusters which contribute to the quasielastic scattering in the form of a Lorentzian squared [Eq. (4)]. Since the average moment is being reduced, so would the spin-wave stiffness as is observed in Figs. 9 and 10. Also the integrated intensity would no longer be described by a Lorentzian but a power law $Q^{-\alpha}$, because of the mixture of the Q^{-2} behavior from the spin waves and the Q^{-4} from the Lorentzian-squared form. This is precisely what is observed between $T_c^{\rm inv}$ and 300 K as demonstrated by the change in α (Fig. 5). From the bulk measurements it appears that at $T_c^{\rm inv}$ the ferromagnetism has completely disappeared. At this temperature the system should be composed of only finite clusters which are too small to support FM behavior. This is shown in our results by the appearance of a finite κ which increases as T decreases (Fig. 4). Only at temperatures below 100 K does κ become significantly larger than our resolution. It also explains why the temperature at which the maximum of intensity appears is strongly Q dependent. Since the breakup of the large FM network results in scattering, following, in part, Eq. (4), the maximum appears at $\kappa=Q/\sqrt{3}$. Since κ varies with temperature the peak in the scattering will appear at different temperatures for different Q values.

Fe-Al differs from all other RSG's in that the bulk susceptibility[11] measurements and Mössbauer[15] studies show that a reentrant PM state exists in the temperature interval between $T_c^{\rm inv}$ and T_f. Below $T_c^{\rm inv}$ the spins are still fluctuating but presumably at a time scale much longer than for $T>T_c$. Only at T_f should the spins freeze. In the present and earlier neutron studies[16,17] no anomaly was observed at T_f. This could be due to the fact that the spins have slowed down sufficiently such that the present resolution ($\delta E=30$ μeV) is too coarse to observe the additional slowing down which would accompany the freezing of the spins at T_f. At the lowest temperature the system is composed of only finite clusters and the scattering follows a Lorentzian behavior.

One of the most unique observations in the present experiments is the thermal hysteresis and the time dependence of scattering observed near $T_c^{\rm inv}$ as shown in Figs. 2 and 6. This behavior is consistent with the appearance of clusters. In our picture, at low temperatures the system is composed of only finite clusters. As we heat it quickly to above $T_c^{\rm inv}$, the FM clusters start to form. If we assume an Arrhenius relation for the formation of the clusters, the energy barrier E_B for their formation would be proportional to the surface area of the cluster, $E_B\sim d^2\sim Q^{-2}$ since $Q=2\pi/d$. This relation implies that $\ln t^*\sim Q^{-2}$ which is the Q dependence observed in Fig. 7.

Our SANS results are qualitatively similar to those of

Child.[17] However, the Q dependence of our scattering differs from that of his. He claims that the scattering follows a Lorentzian-squared form at all temperatures. As shown above, the line shape is changing with temperature. Also, Child reported a maximum in κ at 160 K and a decrease at lower and high temperatures. This is quite different from the present study where κ is resolution limited over the temperature range 100—500 K.

In conclusion, we have measured small-angle total neutron scattering and inelastic scattering of the ordered $Fe_{0.7}Al_{0.3}$ alloy in the temperature regions where bulk measurements suggest a peculiar sequence of transitions. Spin-wave, quasielastic, and small-angle—scattering behavior indicates that the sequence of phase transitions is driven by the interaction of two magnetically separated groups of spins. Future work will include a study of the field dependence and also similar measurements on different concentrations of iron.

ACKNOWLEDGMENTS

We appreciate the assistance provided by G. Aeppli in using programs for data analysis and the extended discussions about the effects of random fields. One of the authors (K.M.) expresses his appreciation to the Brookhaven National Laboratory Neutron Scattering group for their hospitality during his stay. This work was carried out as a part of U. S.—Japan Cooperative Neutron Scattering Program. Work at Brookhaven National Laboratory was supported by the Division of Materials Science, U. S. Department of Energy, under Contract No. DE-AC02-76CH00016.

---

*Present address: Institute for Solid State Physics, University of Tokyo, 7-22-1 Rappongi, Minato-ku, Tokyo 106, Japan.

†Present address: Department of Physics, Faculty of Liberal Arts, Shinshu University, Matsumoto 390, Japan.

[1]D. Sherrington and S. Kirkpatrick, Phys. Rev. Lett. 35, 1792 (1975).

[2]B. H. Verbeek, G. J. Nieuwenhuys, H. Stocker, and J. A. Mydosh, Phys. Rev. Lett. 40, 586 (1978).

[3]S. K. Burke, R. Cywinski, and B. D. Rainford, J. Appl. Crystallogr. 11, 644 (1978).

[4]M. B. Salamon, K. V. Rao, and H. S. Chen, Phys. Rev. Lett. 44, 596 (1980).

[5]S. M. Bhagt, J. A. Geohegan, and H. S. Chen, Solid State Commun. 36, 1 (1980).

[6]H. Maletta and P. Convert, Phys. Rev. Lett. 42, 108 (1979).

[7]A. Arrott and H. Sato, Phys. Rev. 114, 1420 (1959).

[8]H. Sato and A. Arrott, Phys. Rev. 114, 1427 (1959).

[9]J. S. Kouvel, J. Appl. Phys. 30, 313S (1959).

[10]S. J. Pickart and R. Nathans, Phys. Rev. 123, 1163 (1961).

[11]R. D. Shull, H. Okamoto, and P. A. Beck, Solid State Commun. 20, 863 (1976).

[12]P. R. Swann, W. R. Duff, and R. M. Fisher, Trans. Metall. Soc. AIME 245, 851 (1969).

[13]H. Okamoto and P. A. Beck, Metall. Trans. 2, 569 (1971).

[14]H. Okamoto and P. A. Beck, Monatsh. Chem. 103, 907 (1972).

[15]G. P. Huffman, in *Amorphous Magnetism,* edited by H. O. Hooper and A. M. de Graaf (Plenum, New York, 1973), p. 283.

[16]J. W. Cable, L. David, and R. Parra, Phys. Rev. B 16, 1132 (1977).

[17]H. R. Child, J. Appl. Phys. 52, 1732 (1981).

[18]K. Motoya, S. M. Shapiro, and Y. Muraoka, Physica 120B, 147 (1983).

[19]S. M. Shapiro, G. Shirane, B. H. Verbeek, G. J. Nieuwenhuys, and J. A. Mydosh, Solid State Commun. 36, 167 (1980).

[20]G. Aeppli, S. M. Shapiro, R. J. Birgeneau, and H. S. Chen, Phys. Rev. B 25, 4882 (1982); 28, 5160 (1983).

[21]Y. Imry and S.-k. Ma, Phys. Rev. Lett. 35, 1399 (1975).

[22]E. Pytte, Y. Imry, and D. Mukamel, Phys. Rev. Lett. 46, 1173 (1981).

[23]K. Binder, Y. Imry, and E. Pytte, Phys. Rev. B 24, 6736 (1981).

[24]H. S. Kogon and D. J. Wallace, J. Phys. A 14, L527 (1981).

[25]H. Yoshizawa, R. A. Cowley, G. Shirane, R. J. Birgeneau, H. J. Guggenheim, and H. Ikeda, Phys. Rev. Lett. 48, 438 (1982).

[26]H. Maletta, G. Aeppli, and S. M. Shapiro, Phys. Rev. Lett. 48, 1490 (1982).

[27]S. M. Shapiro, C. R. Fincher, Jr., A. C. Palumbo, and R. D. Parks, Phys. Rev. B 24, 6661 (1981).

[28]G. Aeppli, S. M. Shapiro, R. J. Birgeneau, and H. Chen (unpublished).

[29]A. B. Harris, Phys. Rev. 175, 674 (1968); 184, 606 (1969).

[30]J. W. Lynn, R. W. Erwin, J. J. Rhyne, and H. S. Chen, J. Appl. Phys. 52, 1738 (1981).

[31]R. E. Walstedt and L. R. Walker, Phys. Rev. Lett. 47, 1624 (1981); C. M. Soukoulis, G. S. Grest, and K. Levin, *ibid.* 50, 80 (1983), and unpublished.